



Publication Year	2018
Acceptance in OA @INAF	2020-11-16T12:28:14Z
Title	Programmable CGH on photochromic material using DMD generated masks
Authors	Alata, Romain; Zamkotsian, Frédéric; Lanzoni, Patrick; PARIANI, Giorgio; Bianco, A.; et al.
DOI	10.1117/12.2292075
Handle	http://hdl.handle.net/20.500.12386/28355
Series	PROCEEDINGS OF SPIE
Number	10546

PROCEEDINGS OF SPIE

SPIDigitalLibrary.org/conference-proceedings-of-spie

Programmable CGH on photochromic material using DMD generated masks

Romain Alata, Frédéric Zamkotsian, Patrick Lanzoni,
Giorgio Pariani, Andrea Bianco, et al.

Romain Alata, Frédéric Zamkotsian, Patrick Lanzoni, Giorgio Pariani, Andrea Bianco, Chiara Bertarelli, "Programmable CGH on photochromic material using DMD generated masks," Proc. SPIE 10546, Emerging Digital Micromirror Device Based Systems and Applications X, 1054606 (22 February 2018); doi: 10.1117/12.2292075

SPIE.

Event: SPIE OPTO, 2018, San Francisco, California, United States

Programmable CGH on photochromic material using DMD generated masks

Romain Alata¹, Frederic Zamkotsian¹, Patrick Lanzoni¹,
Giorgio Pariani², Andrea Bianco², Chiara Bertarelli³

¹ Aix Marseille Université, CNRS, LAM (Laboratoire d'Astrophysique de Marseille), 13388, Marseille, France

² INAF – Osservatorio Astronomico di Brera, Via Bianchi 46, 23807 Merate, Italy

³ Politecnico di Milano, Dipartimento di Chimica, Materiali e Ingegneria, p.zza L. Da Vinci 32, 20133, Milano, Italy

e-mail: frederic.zamkotsian@lam.fr

ABSTRACT

Computer Generated Holograms (CGHs) are used for wavefront shaping and complex optics testing, including aspherical and free-form optics. Today, CGHs are recorded directly with a laser or intermediate masks, allowing only the realization of binary CGHs; they are efficient but can reconstruct only pixilated images. We propose a Digital Micromirror Device (DMD) as a reconfigurable mask, to record rewritable binary and grayscale CGHs on a photochromic plate. The DMD is composed of 2048x1080 individually controllable micro-mirrors, with a pitch of 13.68 μm . This is a real-time reconfigurable mask, perfect for recording CGHs. The photochromic plate is opaque at rest and becomes transparent when it is illuminated with visible light of suitable wavelength. We have successfully recorded the very first amplitude grayscale CGH, in equally spaced levels, so called *stepped CGH*. We recorded up to 1000x1000 pixels CGHs with a contrast greater than 50, using Fresnel as well as Fourier coding scheme. Fresnel's CGH are obtained by calculating the inverse Fresnel transform of the original image at a given focus, ranging from 50cm to 2m. The reconstruction of the recorded images with a 632.8nm He-Ne laser beam leads to images with a high fidelity in shape, intensity, size and location. These results reveal the high potential of this method for generating programmable/rewritable grayscale CGHs, which combine DMDs and photochromic substrates.

Key words: Computer Generated Hologram, CGH, programmable CGH, MOEMS, photochromic material, optical testing, wavefront shaping, DMD.

1. INTRODUCTION

Computer Generated Holograms (CGHs) are useful for wavefront shaping and complex optics testing, including aspherical and free-form optics [1]. CGHs are classified in two groups: 1- phase holograms, which are obtained by recording a phase variation in a material having a modulated refractive index or thickness; 2- amplitude holograms, where an intensity pattern is recorded in a material whose transparency can be locally controlled. Phase and amplitude holograms provide the same performances in terms of image reconstruction quality, but different diffraction efficiency. For instance, binary phase holograms, show 40% diffraction efficiency in the first order, whereas efficiency is limited to 10% for binary amplitude holograms [2]. Therefore, amplitude holograms are usually applied in interferometry, which is not intensity limited.

Grayscale amplitude and grayscale phase holograms are known to give a higher reconstruction quality than binary holograms [2], but they require a more complex production process. Specifically, the production of phase grayscale CGHs is complex since a series of masks has to be consecutively aligned very precisely, and a developing step is required after each exposure step to obtain the final hologram.

To our best knowledge, only grayscale phase CGHs have been obtained so far by micro-lithography [3], the uniformity of the material thickness being the main limiting parameter for these components [4]. Concerning amplitude CGHs, they are nowadays produced in chrome on glass by means of lithographic techniques, either mask or maskless (by direct writing) lithography. Due to the binary nature of the chrome developing process, these techniques allow for easily writing binary CGHs, but they cannot provide grayscale CGHs.

In this paper, we demonstrate an original recording technique, which makes use of a programmable mask and a non-threshold photosensitive material, to produce ready to use grayscale CGHs in a one exposure process without requiring any developing step. Indeed, a set-up based on a Digital Micro-mirror Device (DMD), which has been originally developed to generate programmable slit masks in multi-object spectrographs [5], is considered. DMDs are programmable devices, composed of millions of micro-mirrors reconfigurable in real time. Actually, DMDs have been extensively used to generate dynamic binary or grayscale holograms [6], by exploiting the fast switching of the mirrors at frequencies higher than the human vision frame rate. The grayscale originates as a dynamic effect and not as a steady state effect. However, the discrete structure of the device induces a high scattering and background noise from the mirrors edges when illuminated with laser light [7], making such holograms useless for interferometry and metrology. Nevertheless, DMDs perfectly reproduce binary masks to be projected with incoherent light on photosensitive plates, thus producing amplitude CGHs. In this work, such plate consists in a photochromic film that can be reversibly converted from an opaque and colored form to a transparent form upon exposure with light of suitable wavelengths [8].

Actually, reversible holograms have been already obtained with photochromic materials [9, 10] and real-time photochromic holograms were shown, by exploiting the fast transition of imidazole dimers [11, 12]. Moreover, photochromic binary CGHs for optical testing have been recently demonstrated [13]. In photochromic materials, a ready to use hologram is generated just after the light exposure, and the reversibility of the photoconversion makes devices rewritable. Even more interesting, the transparency of a photochromic layer can be tuned by the dose of light absorbed, which opens to the development of grayscale patterns [14]. In fact, the DMD set-up allows for easily recording grayscale CGHs with equidistant transparency levels, named as *stepped CGHs*, in a single exposure process. The lower diffraction efficiency of grayscale amplitude holograms with respect to binary amplitude holograms (6% vs. 10% [2]) is here compensated by a better image reconstruction quality, an easy exposure process and no developing steps, which are the limiting factors in the production of grayscale phase holograms.

In this paper, we report on the first stepped CGHs and results are compared to binary CGHs. We read the recorded information using a low power 632.8 nm laser, and the whole hologram is erased with a UV flash, for a reusable substrate.

2. RECORDING AND RECONSTRUCTION OF A CGH

We developed 2 set-ups, respectively dedicated to the recording of the calculated CGH and the reconstruction of the original encoded images.

2.1 Recording set-up

Figure 1 shows our first set-up, dedicated to the CGH recording on the photosensitive plate. The DMD, controlled by the formatter board [15] is illuminated by a collimated beam from a white source, and redirects the light toward the plate. The beam is illuminating the entire DMD and the light power is homogeneous on the plate. The pattern reproduced by the DMD has to be projected onto the plate as precisely as possible, so the plate is illuminated through an Offner relay with a magnification of 1:1. This relay provides a nearly aberration free beam and has the advantage of being compact. The unit magnification means that the maximum size of CGH is directly limited by the size of the DMD; the micro-mirrors of the DMD therefore correspond to the “pixels” of the CGH. Finally, a post-CGH imaging system located right after the CGH plate consists of two lenses, a filter around 600 nm and a CCD camera. This system in an afocal assembly allows imaging of the CGH during writing, in situ and in real time. Magnification is tuned by changing properly the pair of lenses, from a value of 1 up to 4.

DMD, CGH and camera planes are then conjugated. Note that DMD plane is a tilted focal plane due to the nature of micro-mirror array: each micro-mirrors tilts out of the array plane by 12° , leading to a global 24° tilted focal plane. This effect is reproduced as well at the post-CGH imaging camera level (the camera plane is tilted by 24°).

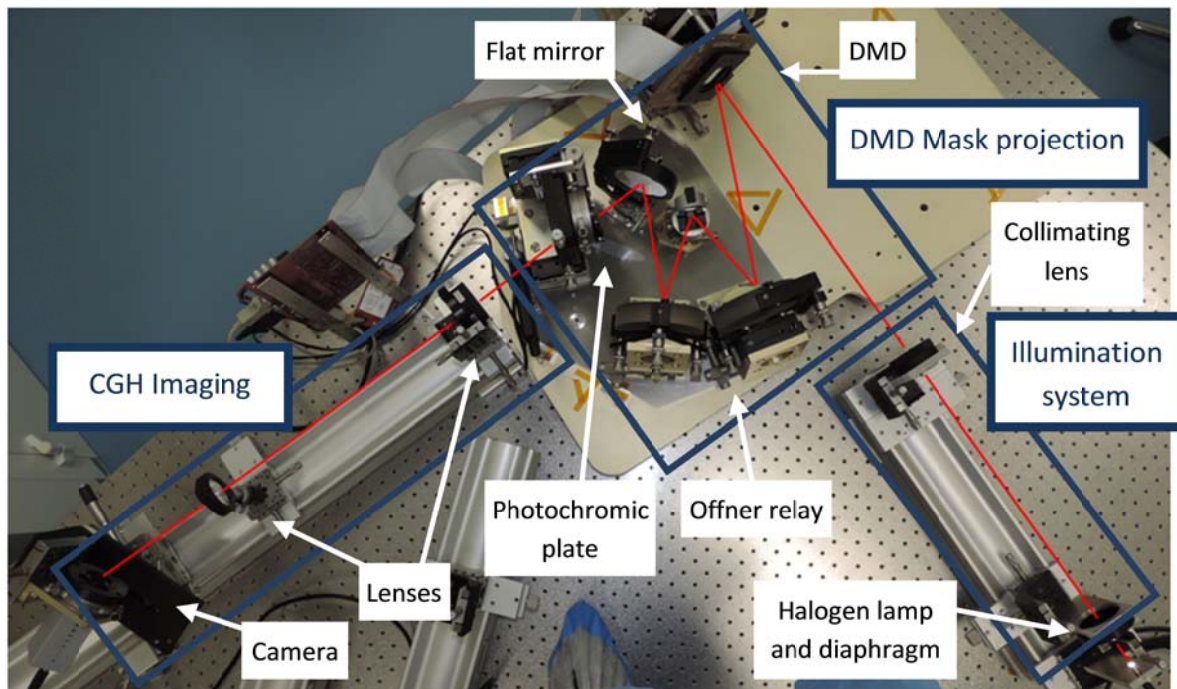


Fig. 1: Picture of the set-up dedicated to CGHs recording; it is based on an illumination unit towards the DMD, an imaging optical system based on a 1:1 magnification Offner relay from the DMD plane to the CGH plane, and a post-CGH imaging system.

2.1.1 Mask generator

Digital Micromirror Devices (DMD) from Texas Instruments could act as reconfigurable mask generator. The largest DMD chip developed by TI features 2048 x 1080 mirrors on a $13.68\mu\text{m}$ pitch, where each mirror can be independently switched between an ON ($+12^\circ$) position and an OFF (-12°) position (Fig. 2). This component has been extensively studied in the framework of an ESA technical assessment of using this DMD component (2048 x 1080 mirrors) for space applications (for example in EUCLID mission). Specialized driving electronics and a cold temperature test set-up have been developed. Our tests reveal that the DMD remains fully operational at -40°C and in vacuum. A 1038 hours life test in space survey conditions (-40°C and vacuum) has been successfully completed. Total Ionizing Dose (TID) radiation tests, thermal cycling (over 500 cycles between room temperature and cold temperature, on a non-operating device) and vibration and shock tests have also been done; no degradation is observed from the optical measurements. **These results do not reveal any concerns regarding the ability of the DMD to meet environmental space requirements [15].**

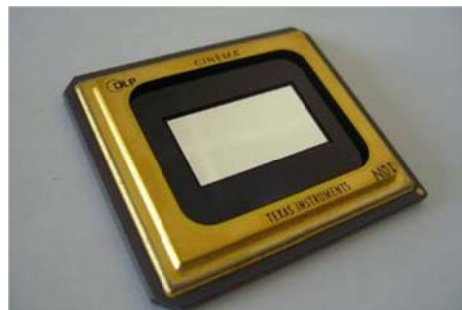


Fig. 2: DMD chip from Texas Instruments (2048 x 1080 micromirrors).

2.1.2 DMD mask projection

A simple imaging Offner-type layout has been set up, based on two identical spherical concave mirrors and a convex mirror (Fig. 3). Indeed, spherical mirrors belong to the same mother mirror, sharing the same radius and center of curvature. One mirror only could be used instead of two separate ones, helping the alignment of the system. However, mechanical and operational constraints can lead to split these two mirrors. We have preferred two identical spherical mirrors with a diameter of 160mm and a radius of curvature of 438mm. The convex mirror has a 224mm radius of curvature. [16]

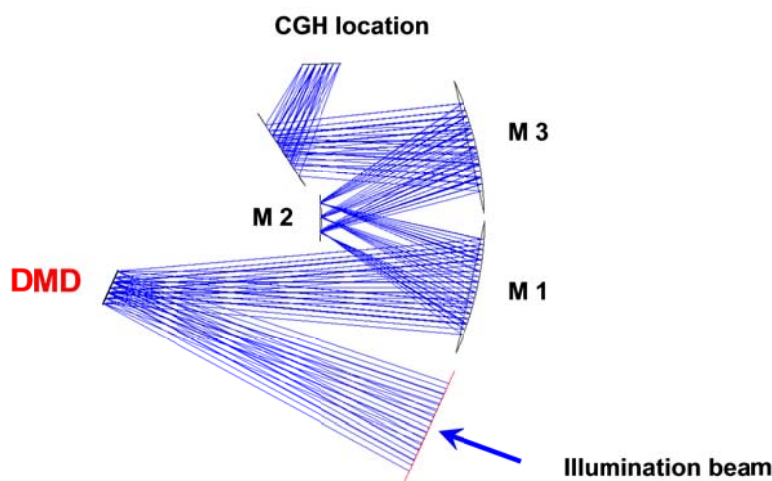


Fig. 3: Optical layout of the imaging set-up.

This optical layout will make the system simple and efficient. Additionally it will not suffer from chromatic aberrations. Delivered image quality onto the CGH plane is high enough to not degrade spatial resolution as shown in Fig. 4. Typical monochromatic spot diameters are $<20\mu\text{m}$ over the whole FOV for wavelengths between 400nm and 800nm; in Fig. 4, boxes are $70\times 70\mu\text{m}^2$.

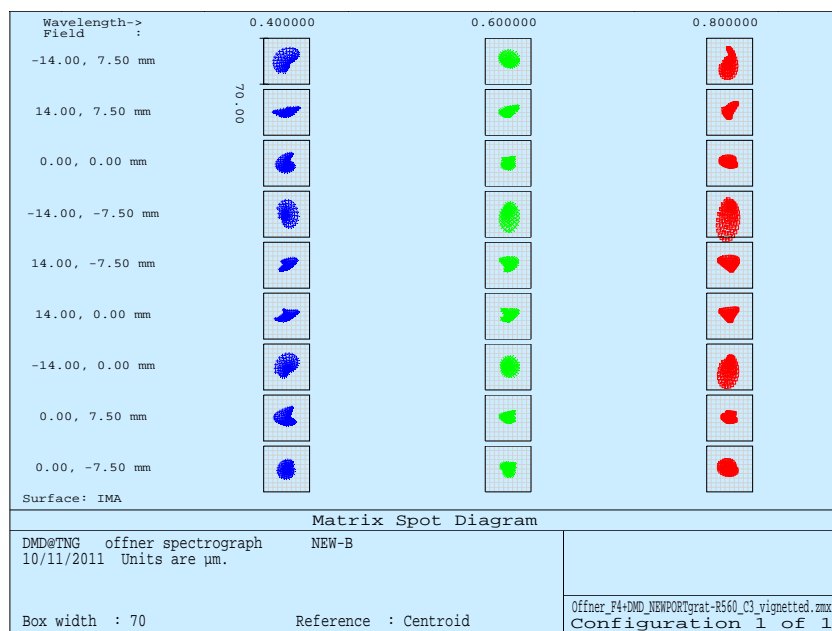


Fig. 4: Imagery spot diagrams. Boxes are $70\times 70\mu\text{m}^2$.

Different wavelengths and field of views are given, covering the whole DMD active surface.

2.2 Reconstruction set-up

The second set-up, shown in Fig. 5, is dedicated to CGH reconstruction. The source is a collimated 632.8 nm He-Ne laser. The camera, placed at the distance z from the plate, is illuminated through the CGH. As described in the next section, the Fresnel holograms are directly calculated from the propagation equations of light, and they are for a given focus. It is thus not necessary to add a lens between the plate and the camera to reconstruct the image, unlike with the Fourier holograms. This is why the source should be rigorously collimated, because a variation in the quality of the collimation can displace the focal plane along the optical axis and change the size of the encoded image.

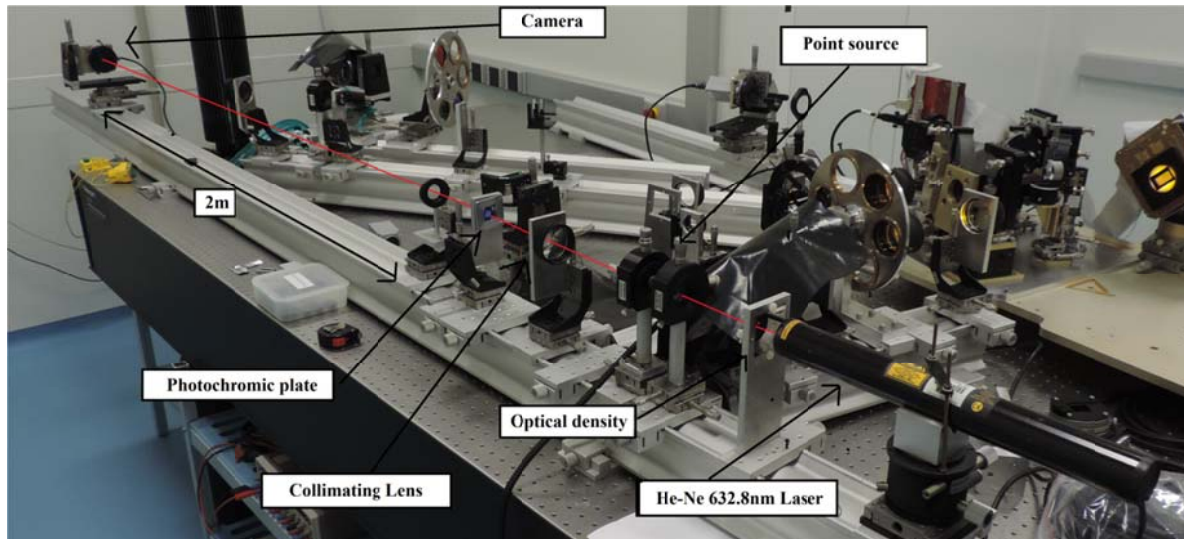


Fig. 5: Picture of the set-up dedicated to image reconstruction, including a 632.8 nm He-Ne laser, the CGH plane and the camera located at the hologram projection distance (2m in this case).

3. PHOTOCHROMIC PLATES

The photosensitive material is a diarylethene-based polyurethane [17]. Such kind of photochromic substrate contains a large content of photochromic units (i.e. 50% wt. in this work) that turns into a high contrast between the colored and uncolored forms, also for thin films. This layer can be reversibly converted from an opaque and colored form to a transparent form upon exposure with light of suitable wavelengths, around 600nm (Fig. 6)

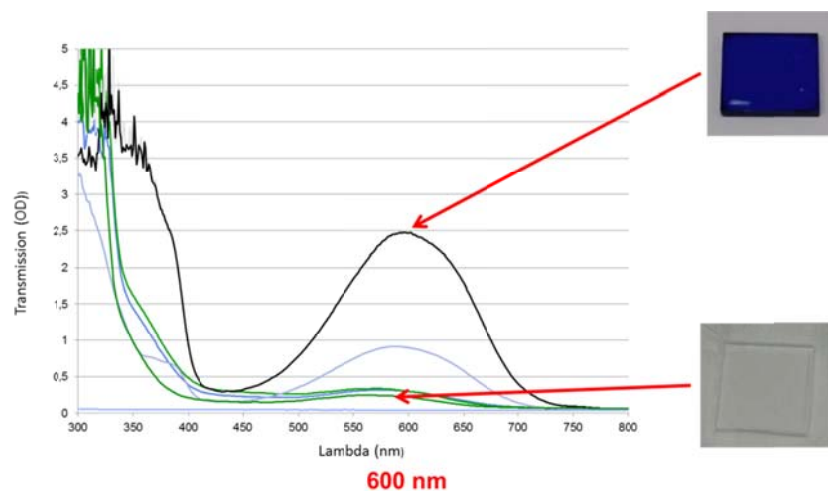


Figure 6: Transmission (Optical Density) of the photochromic material used in the UV-Visible range of the spectrum showing the opaque to the transparent states, according to the illumination amount of the plate

Moreover, the optical quality in terms of transparency and scattering is very good. The photochromic plate is 3 μ m thick and the film is set uniformly to the opaque state by a UV exposure. The conversion under light illumination of the photochromic film has been previously determined by a kinetic model that provides the degree of transparency as function of the film features and illumination conditions [14].

4. CGHs CALCULATION

CGHs could be calculated as Fourier holograms and Fresnel holograms. In this paper we will focus on Fresnel CGHs.

4.1 Fourier holograms

Fourier holograms are obtained using algorithms encoding the inverse Fourier transform of the wavefront to be reproduced. These algorithms [18, 19, 20] are operating in a common way. Once the inverse Fourier transform is calculated, the complex information contained in each pixel is encoded in a cell of WxH pixels, W and H depending on the used algorithm. The number of pixels of a Fourier hologram is therefore necessarily larger than the number of pixels defining the image. This leads to limiting the resolution and size of images to be encoded. The DMD is composed of 2048x1080 micro mirrors and the dimensions W and H being 4 pixels or larger, with the most compact algorithm, the maximum attainable resolution of the image to be encoded is 250x250 pixels, and its actual size is limited to 3,4x3.4mm. Since these holograms are based on the Fourier transform, it is necessary to add a lens after the CGH in the reconstruction set-up, for applying the optical Fourier transform to the CGH, and display the image. Fourier holograms could be calculated very fast but they will not be discussed in this paper.

4.2 Fresnel holograms

Fresnel holograms are directly calculated with the light propagation equations, and can be modeled by the Rayleigh - Sommerfeld integral diffraction given in equation 1 [21].

$$A_z(x, y) = \frac{A_0}{i\lambda} \iint t(u, v) \frac{e^{ikr}}{r} \cos(\theta) du dv \quad (1)$$

The resulting complex wave A_z is estimated by calculating the sum of the contributions of each pixel of the hologram anywhere on the screen located at a distance z . Each pixel is considered as a secondary spherical wave source weighted by the transmittance $t(x, y)$ of the hologram. These secondary waves are generated when the incident wave, characterized by its complex amplitude A_0 and its wavelength λ (or the wave number $k = 2\pi/\lambda$), reaches the hologram. The angle θ is the skew factor and is equal to zero in our configuration.

The distance z between the hologram and the screen being much greater than the dimensions of the detector and CGH dimensions, the equation (1) can be approximated by the following 2D convolution product :

$$A_z(x, y) = A_0(x, y) e^{ikz} t * h_z \quad (2)$$

Where the kernel convolution h_z , called Fresnel function, is:

$$h_z(x, y) = \frac{1}{i\lambda z} e^{(i\pi \frac{x^2+y^2}{\lambda z})} \quad (3)$$

The equation (2) simulates the diffraction of the reference wave on the hologram and thus reconstructs the digitally encoded image, the development of this reconstruction being obtained by estimating the convolution kernel h_z at the desired focal length z .

The convolution function is defined by the equation (4):

$$a(x, y) = \iint b(u, v). c(x - u, y - v) du dv = b * c \quad (4)$$

5. BINARY CGH

The first object to be recorded on the plate is the binary CGH of the letter "Z", formed on a 10x10 pixel grid as shown on Fig 7(a), with a physical size of 2x2mm² and calculated at a focus of 2m. As the photosensitive material does not fully cover the 1 inch square support plate, a maximum CGH dimension of 1cmx1cm has been fixed, which leads to a CGH resolution of 720x720 pixels. The physical dimensions of the "Z" are fixed as 1/5 of the CGH dimensions. The object, smaller than the CGH, is surrounded by the Fresnel lens pattern. With a longer CGH the resolution may become insufficient because the fringes on the corner will be too close.

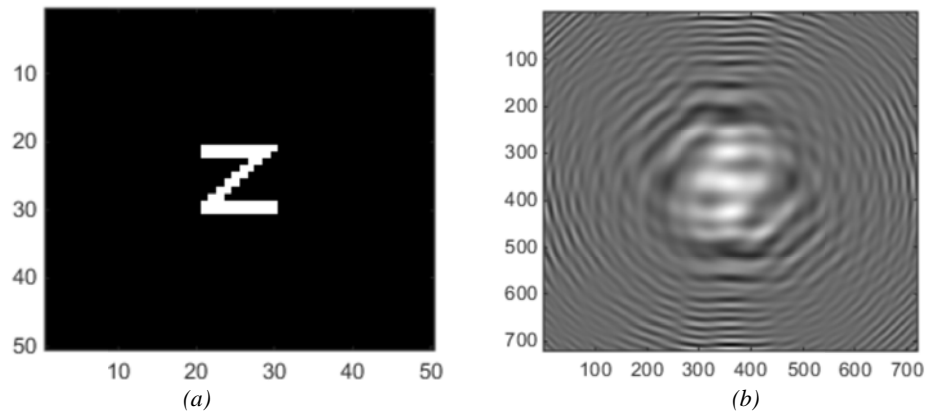


Fig. 7: (a) Original image to be encoded; a 10x10pixels "Z"
(b) 720x720 pixels calculated continuous CGH, for an image dimension of $2 \times 2 \text{ mm}^2$ at a focus of 2m

Usually, when the recording method is based on a physical mask or a laser, the CGH is binarized. Figure 8a represents the binary CGH obtained for our image, and in Fig. 8b, the pattern recorded on the plate by using our recording set-up presented in the previous section is shown. The recorded hologram is a faithful reproduction of the simulated one. The vignetting effect seen on this image was due to the post-CGH imaging mount and has been corrected in the next paragraphs.

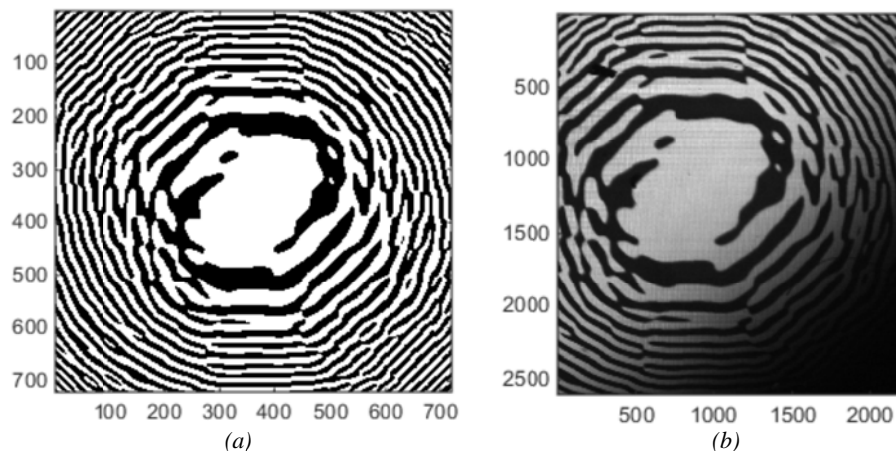


Fig. 8: (a) 720x720 pixels calculated binary CGH and (b) actual pattern recorded on the plate

We can also simulate the reconstructed image by applying the direct transformation of the binary Fresnel CGH, which allows us to check the reliability of the code (Fig. 9a).

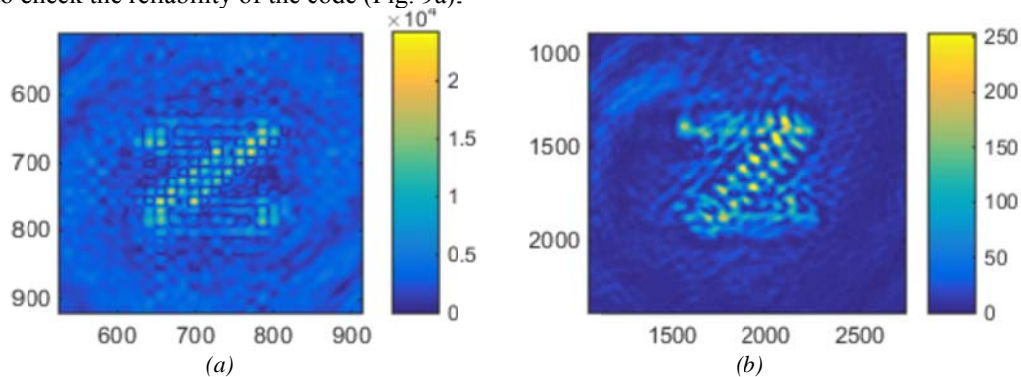


Fig. 9: Reconstruction of a 720x720 pixels CGH of a 10x10 pixels "Z" of $2 \times 2 \text{ mm}^2$ at 2m :
(a) Simulation and (b) Real reconstruction

In Fig. 9b is shown the reconstructed image, identical to the simulated one. It shows the quality of our recording and reconstruction set-ups. However, the obtained image does not completely look like the original image (Fig. 7a). Binary CGHs do not well suit the shape and the intensity of the calculated continuous CGH. It follows that reconstructed images from a binary CGH are either pixilated or “empty” with a thin boundary (high spatial frequencies), depending on the ratio between the focus and the image size.

6. STEPPED CGH

In the present configuration, recording a binary CGH requires the projection of a single mask set on the DMD to the photochromic plate, for an exposure time large enough to produce the full conversion of the opaque form into the transparent form of the illuminated pixels. The use of a series of defined binary masks, which are sequentially projected on the photochromic plate, creating for each step a new degree of transparency, allows for obtaining stepped CGHs. It is worth noting that the production of grayscale CGHs does not require longer time than recording binary CGHs since the maximum transparency that can be achieved in a grayscale CGH corresponds to the full transparency in the binary CGH.

6.1 Illumination law

As described in paragraph 3, the photochromic material becomes progressively transparent when illuminated by visible light. This means that a given level of transparency, i.e. a given level of gray, corresponds to a given exposure time. But the response of the material is not linear and has to be characterized. Our recording set-up could take images of the plate during the recording, thanks to the post-CGH camera. Therefore we enlightened the plate, and took images every 30 seconds to plot the photochromic plate time response shown in Fig. 10a. This curve, called illumination law, gives the transparency of the plate as a function of exposure time. Specifically, it is the illumination law that will be followed to finely control the transparency of the plate. This law has been obtained for a given light power, but it has been verified that it can be rescaled with a homothetic transformation in order to obtain the right illumination curve for another light power.

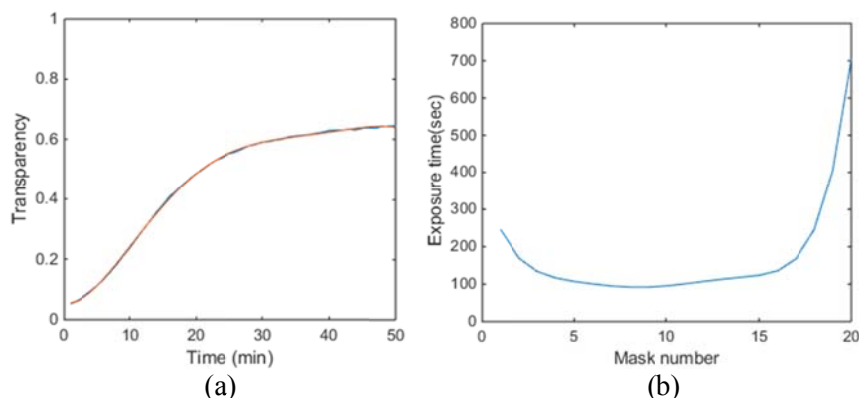


Fig. 10: (a) Illumination law of the photochromic plate
(b) Exposure time of each mask when the CGH is stepped in 20 levels

A binary CGH can easily be recorded with our set-up; it simply requires displaying it on the DMD and to project it on the plate during the required time. While recording a stepped CGH, a serial of binary mask has to be defined, with the adequate exposure time for each of them. We decided to discretize the CGH in 20 gray levels, this number of steps is sufficient as the difference between the continuous and stepped CGH falls then below 1%. Twenty binary masks are calculated by binarizing the continuous CGH pattern with thresholds ranging from 0 to 1 in steps of 0.05. Once the serial of mask is obtained, each exposure time is deducted from the illumination law show in Fig. 10a. The curve shown in Fig. 10b gives the exposure time for each mask. They range from 1min 32sec up to 11min 43sec.

6.2 Mask generation

Figure 11 illustrates the recording strategy using the example of a detail of the 10x10 pixels “Z” CGH. Each mask is displayed during its own exposure time to reach the following discrete level of transparency. We can see that the darker areas are illuminated with the first masks only, while the most transparent areas are illuminated through almost all remaining masks. 20 masks have been calculated, Fig. 11 shows 7 of them with the theoretical stepped CGHs image where it is possible to identify all steps.

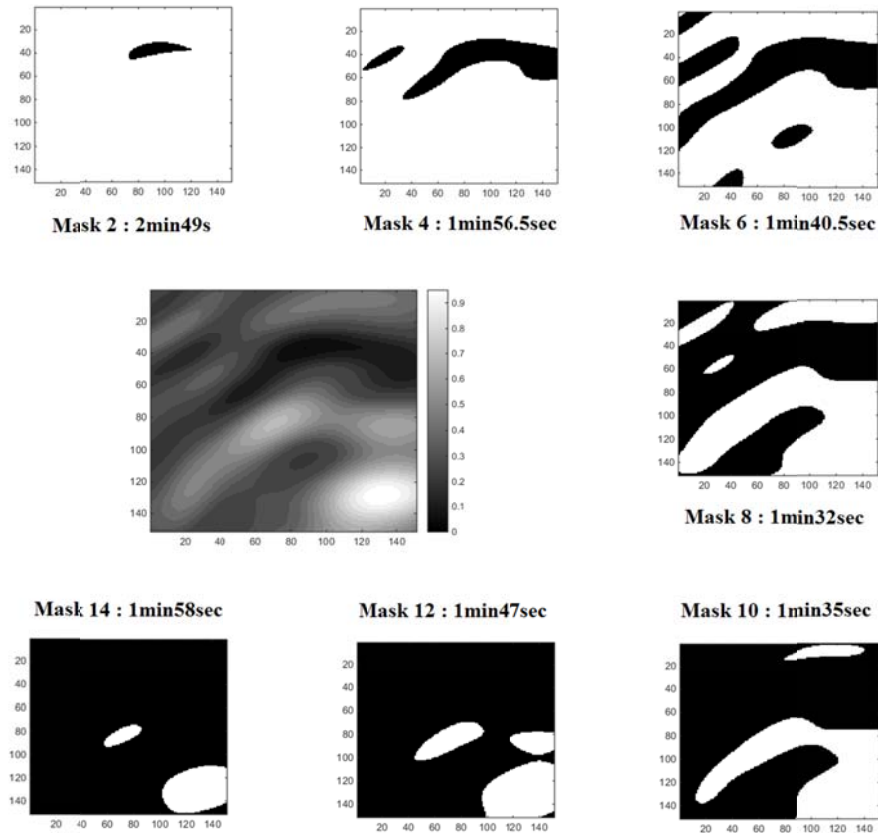


Fig. 11: Recording strategy: detail of the CGH and the corresponding 7 masks out of the serial of 20 masks

This method has already been used on phase CGH but with a low quality result due to critical issues like the good alignment of successive masks. With a DMD, this problem obviously disappears since the position error between 2 consecutive masks is null; in addition, it is instantaneous to apply the consecutive masks.

6.3 Stepped CGHs recording

We have been able, thanks to the method described above, to get the CGH on Fig. 12b. It corresponds to the CGH calculated (Fig. 12a) for a 200x200 pixels "Z" of a size of 2x2mm located at 2m and stepped into 20 levels.

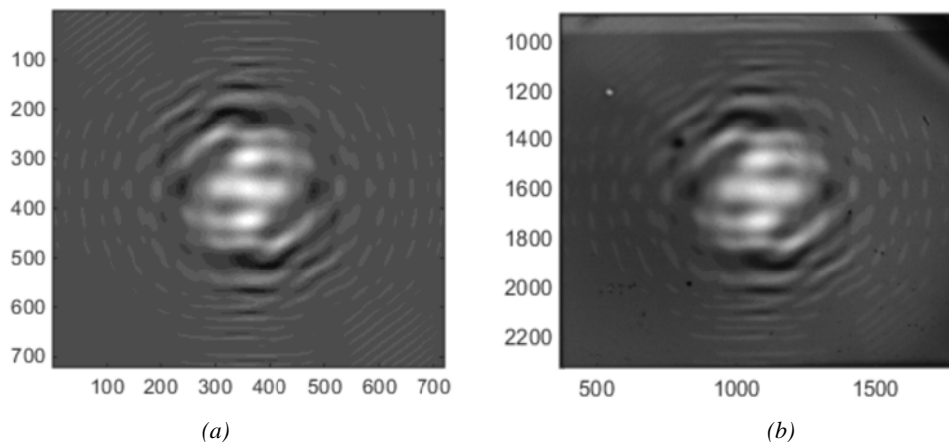


Fig. 12: 720x720 pixels stepped CGH, of a 200x200 pixels "Z" of 2x2mm at a focus of 2m:
(a) calculated; (b) recorded

To be sure that the zones correspond to our expectations, the contours of the theoretical stepped CGH are displayed on the real one as shown in Fig.13. It represents a small area of the CGH, obtained with an optical magnification of 1:3.75; the contours (black lines) correspond to the limit between the level 7 and 8 in the theoretical CGH and it is exactly at the right place on the real one, while red arrows show that even a single mirror shift is visible and has been written properly on the plate.

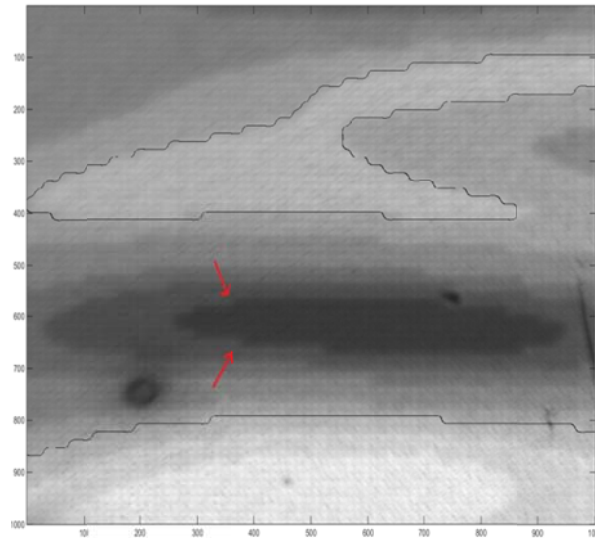


Fig. 13 : Magnification of a part of the written CGH; with contours and arrows showing the high resolution of the recorded CGH

Figure 13 shows the precision of our recording technique. Each micro-mirror is clearly identifiable and each zone is perfectly defined. The fact that the pattern of the DMD is visible on the plate could have been a source of additional noise, but after verification (both calculation and measurement) it has actually no measurable impact. It would have been possible to remove this high frequency pattern with a *sub-pixel dithering* strategy. The principle is to slightly shift the plate at different positions during the exposure with a pitch smaller than a pixel. This technique allows smoothing the CGH, and then makes the high frequency pattern due to the DMD disappear.

The contrast of the CGH, which is closely related to the diffraction efficiency of amplitude holograms [13], has been evaluated directly with the imaging set-up on the CGH plate. The contrast is calculated as the ratio between the transmittance of the transparent areas over the transmittance of the colored areas measured by the CCD. The linearity of CCD has been checked and light intensity has been calibrated in order to have a good S/N for all the recorded images independently from the transparency degree. A contrast equal to 50 was obtained at 610 nm (10 nm bandwidth), which turns into a diffraction efficiency of the order of 75% of the maximum diffraction efficiency (achieved for infinite contrast). It is worth noting that higher contrasts can be reached by optimizing the photochromic plate (i.e. thickness, content and structure of the photoactive units).

The illumination law has been verified: the mean of each level has been calculated independently on pixels sample number larger than 10^5 . The obtained curve is linear, with a standard deviation of 1.4%.

6.4 Stepped CGHs reconstruction

Figure 14 shows the simulated reconstructed image and the actual reconstructed image using our second set-up (paragraph 2.2). The image dimension on the camera is 570x570 pixels, which gives a physical size of 2x2mm as expected. [22]

A shadow appears on the upper left hand side of the experimentally reconstructed image, it corresponds to the diffraction caused by a defect on the CGH plate, visible in Fig. 12b. Fresnel CGHs are very sensitive to defects and cannot be reconstructed correctly if the most transparent areas are altered. The image size and the focus chosen for the calculation also depend on the quality of the illumination. If the laser beam converges instead of being well collimated, the focus

will be shorter and the size of the image smaller, and vice versa if the laser beam is diverging. Note also in figure 14b interference fringes probably due to multiple reflections in the plate itself.

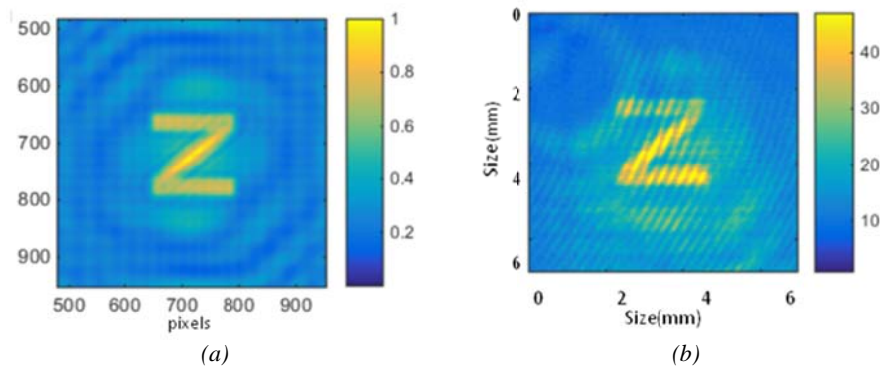


Fig. 14: Reconstruction of a 720x720 pixels stepped CGH, of a 200x200 pixels “Z” of 2x2mm at a focus of 2m
 (a) Simulation of the reconstruction from theoretical CGH
 (b) Real reconstruction of the image

As resulting from the simulation, the reconstructed image (Fig. 14b) is very faithful to the original image (Fig. 7a), meaning that grayscale CGHs clearly give better reconstructed images than binary CGHs.

7. STEPPED CGH - FRESNEL LENS

In order to simulate a phase-like device, a Fresnel lens is designed, calculated, realized and tested. A Fresnel lens is a plane-convex lens chopped in annular rings for reducing the volume and mass of the lens while keeping a short focal distance (Fig. 15a).

In order to generate a Fresnel lens, the original image to be encoded is a point source, but we chose instead a uniform disk of 200 pixels in diameter (Fig. 15b) for making a larger object to characterize after the image reconstruction process; we will be then able to show the ability of our method to generate efficient Fresnel lenses. The obtained lens does not look like as a typical Fresnel lens, but still keeps the typical ring features (Fig. 15c).

The Fresnel CGH is calculated as described in paragraph 4, with as input, a uniform disk of 2mm in diameter, located at 2m of the lens. The CGH is defined in grayscale on a circular shape with a size of 10mm (720 pixels), and divided in amplitude into 20 steps.

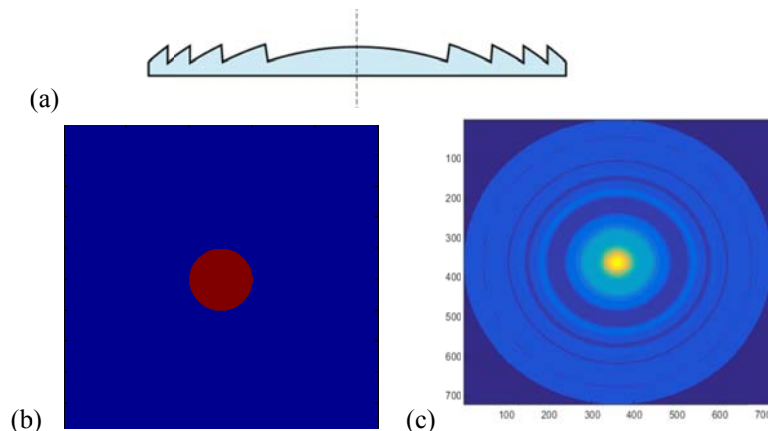


Fig. 15: (a) Schematic view of a Fresnel lens
 (b) Original image to be encoded; a 200pixels uniform disk
 (c) Simulation of 720x720 pixels stepped CGH, of a 200pixels uniform disk of 2mm at a focus of 2m

The CGH – Fresnel lens is recorded on a photochromic plate with the method described above and the result is shown in Fig. 16. The CGH is stepped into 20 levels and magnification of different parts of the CGH reveals the different features written with high accuracy. Note that the CGH has a circular shape in order to match perfectly with a Fresnel-like lens. The reconstructed image might then be “cleaner”.

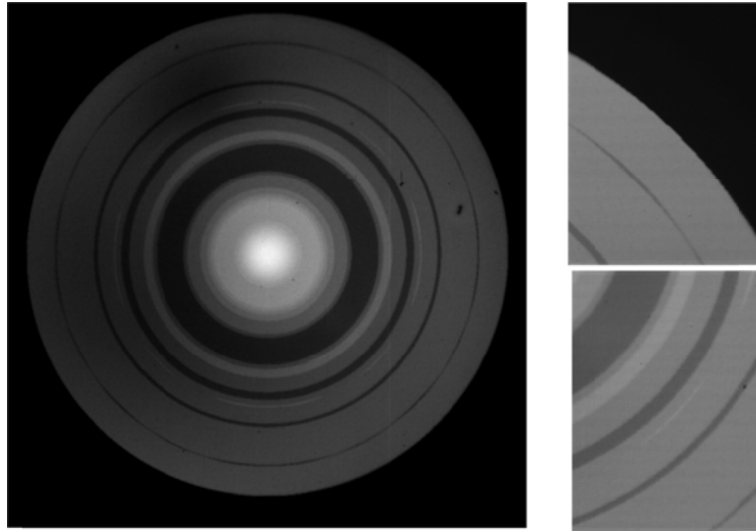


Fig. 16: Recorded CGH - Fresnel lens on the photochromic plate
Magnification of parts of the written CGH

Figure 17 shows the simulated reconstructed image and the actual reconstructed image using our second set-up (paragraph 2.2). The physical size of the disk is exactly 2mm in diameter as expected. The simulated image has been produced from the actual image of the CGH, taking then into account possible imperfections of the recorded hologram. Note also in figure 17b interference fringes probably due to multiple reflections in the plate itself.

The reconstructed image (Fig. 17b) is very faithful to the original image (Fig. 15a), meaning that grayscale CGHs –Fresnel lenses could be designed, recorded and used with high efficiency.

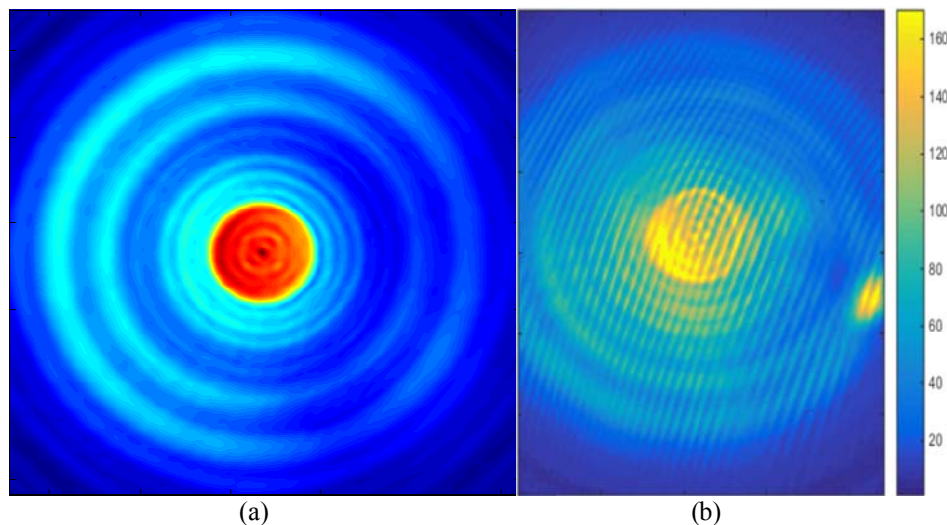


Fig. 17: Reconstruction of a 720 pixels in diameter stepped CGH, of a 200 pixels uniform disk of 2mm at a focus of 2m
(a) Simulation of the reconstruction from actual CGH – Fresnel lens
(b) Real reconstruction of the image

8. CONCLUSION

Computer generated holograms are well suited for optical testing and wavefront shaping. Up to now amplitude holograms have only been recorded in binary format, and our method increases their quality by enabling the realization of stepped holograms with discrete gray levels.

We have been able to successfully record several Fresnel CGHs, with stepped and binary coding. The resolution of recorded holograms was set to 720x720 pixels to be able to project it on the functional part of the photochromic plate, up to 1x1cm² size. The high optical resolution of our set-up allowed making high quality recorded CGH with the desired grayscale properly produced. The reconstructed images using stepped holograms are very faithful to the original images without being pixilated as for binary holograms.

The next step will be to code wavefronts containing phase information. We also plan to conduct the same study on Fourier holograms as they are much faster to compute and may give better results according to preliminary simulations. Finally, we will also use our method to create beam shapers including apodizers, using the same protocol as for stepped CGHs.

ACKNOWLEDGMENTS

This work has been partly funded by the European Union FP7-OPTICON 2 program.

REFERENCES

- [1] C. Pruss, S. Reichelt, H. J. Tiziani and W. Osten, "Computer-generated holograms in interferometric testing," *Opt. Eng.* **43** (11), 2534-2540 (2004)
- [2] Brown, B. R. and Lohmann, A. W., "Computer-generated Binary Holograms," *IBM J. Res. Dev.* (1969)
- [3] Y-T. Lu, C-S. Chu, H-Y. Lin, "Characterization of the gray-scale photolithography with high-resolution gray steps for precise fabrication of diffractive optics," *Opt. Eng.* **43**(11) 2666-2670 (2004)
- [4] N. Luo, Y. Gao, S. He, Y. Rao, "Research on exposure model for DMD-based digital gray-tone mask," *Proc SPIE Vol. 7657*, 7657 12-1 (2010)
- [5] F. Zamkotsian, P. Spano, P. Lanzoni, H. Ramarijaona, M. Moschetti, M. Riva, et al., "BATMAN: a DMD-based Multi-Object Spectrograph on Galileo telescope," in *Proceedings of the SPIE conference on Astronomical Instrumentation 2014*, *Proc. SPIE* **9147**, Montréal, Canada, (June 2014)
- [6] R.S. Nesbitt, S.L. Smith, R.A. Molnar, S.A. Benton, "Holographic recording using a digital micromirror device," *Proc. SPIE* **3637**, Practical Holography XIII, 12 (March 25, 1999); doi:10.1117/12.343767
- [7] Park, M.-C., Lee, B.-R., Son, J.-Y., Chernyshov, O., "Properties of DMDs for holographic displays," *J. Mod. Opt.* **62**(19), 1600-1607 (2015)
- [8] C. Bertarelli, A. Bianco, R. Castagna and G. Pariani, "Photochromism into optics: Opportunities to develop light-triggered optical elements," *Journal of Photochemistry and Photobiology C: Photochemistry Reviews* **12**(2), 106-125 (2011) doi: 10.1016/j.jphotochemrev.2011.05.003
- [9] Nan Xie, Yi Chen, Baoli Yao, Ming Lie, "Photochromic diarylethene for reversible holographic recording," *Materials Science and Engineering: B*, **138**(3), 210-213 (2007)
- [10] Yi Chen, Congming Wang, Meigong Fan, Baoli Yao, Neimule Menke, "Photochromic fulgide for holographic recording," *Optical Materials*, **26**(1), 75-77 (2004)

- [11] Y. Kobayashi and J. Abe, "Real-Time Dynamic Hologram of a 3D Object with Fast Photochromic Molecules," *Adv. Opt. Mater.* **4**(9), 1354–1357 (2016)
- [12] N. Ishii, T. Kato, and J. Abe, "A real-time dynamic holographic material using a fast photochromic molecule" *Sci. Rep.* **2**, 819 (2012)
- [13] G. Pariani, C. Bertarelli, G. Dassa, A. Bianco, G. Zerbi, "Photochromic polyurethanes for rewritable CGHs in optical testing," *Optics Express* **5** (19), 4536-4541 (2011)
- [14] G. Pariani, A. Bianco, R. Castagna and C. Bertarelli, "Kinetics of photochromic conversion at the solid state: Quantum yield of dithienylethene-based films," *Journal of Physical Chemistry A* **115**(44), 12184-12193 (2011) doi: 10.1021/jp207210p
- [15] F. Zamkotsian, P. Lanzoni, E. Grassi, R. Barette, C. Fabron, K. Tangen, L. Valenziano, L. Marchand, L. Duvet "Successful evaluation for space applications of the 2048x1080 DMD," " in Proceedings of the SPIE conference on MOEMS 2011, *Proc. SPIE* **7932**, San Francisco, USA (2011)
- [16] Frederic Zamkotsian, Harald Ramarijaona, Manuele Moschetti, Patrick Lanzoni, Marco Riva, Nicolas Tchoubaklian, Marc Jaquet, Paolo Spano, William Bon, Romain Alata, Luciano Nicastro, Emilio Molinari, Rosario Cosentino, Adriano Ghedina, Manuel Gonzalez, Walter Boschin, Paolo Di Marcantonio, Igor Coretti, Roberto Cirami, Filippo Zerbi, Luca Valenziano, "Building BATMAN: a new generation spectro-imager on TNG telescope ", in Proceedings of the SPIE conference on Astronomical Instrumentation 2016, *Proc. SPIE* **9908**, Edinburgh, United Kingdom, (2016)
- [17] G. Pariani, R. Castagna, G. Dassa, S. Hermes, C. Vailati, A. Bianco and C. Bertarelli, "Diarylethene-based photochromic polyurethanes for multistate optical memories," *Journal of Materials Chemistry* **21**(35), 13223-13231 (2011) doi: 10.1039/c1jm11870f
- [18] A. W. Lohmann and S. Sinizinger, "Graphic codes for computer holography," *Appl. Opt.* **34**, 17 (1995)
- [19] C. B. Burckhardt, "A simplification of Lee's method of generating holograms by computers," *Appl. Opt.* **9**, 1949-1959 (1970)
- [20] C. K. Hsueh and A. A. Sawchuk, "Computer-generated double-phase holograms," *App. Pot.* **17**, 3874-3883 (1978)
- [21] L. Denis, PhD Thesis, "Traitement et analyse quantitative d'hologrammes numériques. Interface homme-machine, " Université Jean Monnet - Saint-Etienne, France (2006), hal.archives-ouvertes.fr/tel-00282661
- [22] Romain Alata, Giorgio Pariani, Frederic Zamkotsian, Patrick Lanzoni, Andrea Bianco, Chiara Bertarelli, "Programmable CGH on photochromic plates coded with DMD generated masks", *Optics Express*, Vol. **25**, n° 6, (2017), <https://doi.org/10.1364/OE.25.006945>